Journal of Hazardous Materials 166 (2009) 1201–1209

Contents lists available at ScienceDirect

Journal of Hazardous Materials

journal homepage: www.elsevier.com/locate/jhazmat

Adsorption characteristics of anionic nutrients onto the PP-*g*-AA-Am non-woven fabric prepared by photoinduced graft and subsequent chemical modification

Hyun-Ju Park, Choon-Ki Na*

Department of Environmental Engineering, Mokpo National University, Jeonnam 534-729, South Korea

ARTICLE INFO

Article history:
Received 9 July 2008
Received in revised form 16 October 2008
Accepted 4 December 2008
Available online 9 December 2008

Keywords:
PP-*g*-AA-Am non-woven fabric
Anion exchange
Isotherm
Kinetics
Ion selectivity
Regeneration efficiency

ABSTRACT

PP-*g*-AA-Am non-woven fabric, which possesses anionic exchangeable function, was prepared by chemical modification of carboxyl group in PP-*g*-AA non-woven fabric to amine group using diethylene triamine. Its sorption characteristics for anionic nutrients including isotherm, kinetics, effects of pH and co-anions, and regeneration efficiency were studied by batch sorption experiments. Sorption equilibriums of PO_4-P on PP-*g*-AA-Am fabric were well described by the Langmuir isotherm model, and their sorption energies were ranged between 9.94 and 15.96 kJ/mol indicating an ion exchange process as primary sorption mechanism. Sorption kinetic data fitted with pseudo-second-order kinetic model and indicated that both external and intraparticle diffusion took part in sorption processes. The uptake of PO_4-P by PP-*g*-AA-Am fabric increased with increasing pH of solution and its optimum pH region was in pH $\geq$4, whereas the uptake of NO_3-N and NO_2-N was higher in weak and strong acidic pH region, respectively. The sorption selectivity for anions by PP-*g*-AA-Am fabric was increased in the order: $SO_4 \geq PO_4 > NO_3 > Cl$. The PP-*g*-AA-Am fabric could be regenerated by a simple acid washing process without lowering the sorption capacity or physical durability.

1. Introduction

Recently, pollutants of nitrogen and phosphorous, which are factors of eutrophication, became a social issue relating to environmental problems [1–3]. At present a biological treatment process is a most widely used technique to remove the nutrients from wastewater. As discharge limits of nutrients become more stringent to prevent the eutrophication, however, the demands on an introduction of advanced treatment techniques continue to increase in sewage and wastewater treatment for the appropriate removal of nitrogen and phosphorus. Accordingly, there have been many attempts in developing advanced treatment with the form of a hybrid process, in which electrolysis, membrane separation, chemical coagulation, and adsorption processes are integrated into existing biological treatment process [4–8]. Among these unit processes, adsorption has been found to be superior to other unit processes for advanced treatment hybrid system in terms of initial cost, simplicity of design, ease of operation and insensitivity to climate [9–11]. Various adsorbents have been investigated for the removal of anionic nutrients from aqueous solutions with varying success, e.g. activated carbon and clay mineral [12,13], ferric and aluminum (hydr)oxides [3,14–17], biomass [18], ion exchange resin [19–21]. However, these adsorbents could not be widely used because of lower adsorption capacity, severe competition with coexisting ions, unfeasible regeneration process, or high operating costs. Therefore, highly effective and more economical adsorbents are still needed.

In our previous paper [22], the preparation method of PP-*g*-AA-Am non-woven fabric was reported, using the photoinduced graft polymerization of acrylic acid (AA) onto polypropylene (PP) non-woven fabric followed by the amination of grafted AA through reaction with diethylene triamine (DETA). As compared with a commercial anion exchange resin, superior sorption capacity of the PP-*g*-AA-Am fabric for phosphate and nitrate was also presented. However, sorption properties of anions by the PP-*g*-AA-Am fabric have not been reported previously in detail.

The aim of the present study was to understand the sorption mechanisms for anionic nutrients, particularly phosphate, and to identify the factors that affect the anion sorption capacity of PP-*g*-AA-Am fabric. In this article, the sorption properties of PP-*g*-AA-Am fabric for removal of anionic nutrients from aqueous solution were investigated in batch mode. Sorption isotherms and kinetics were determined and modeled using several equations generally adapted in the literatures to describe experimental data. The effects of pH and coexisting anions on the sorption capacity of PP-*g*-AA-Am fabric were investigated. The regeneration efficiency of PP-*g*-AA-Am fabric was also examined.

* Corresponding author.
E-mail address: nack@mokpo.ac.kr (C.-K. Na).

0304-3894/$ – see front matter © 2008 Elsevier B.V. All rights reserved.
doi:10.1016/j.jhazmat.2008.12.031

2. Experimental

2.1. Materials and reagents

PP non-woven fabric of 180 g/m^2 was used as the substrate polymer for grafting after being cut into pieces of 1 cm × 10 cm and washed with a neutral detergent solution. AA (Daejung Chemical Co., Korea) and benzophenone (BP, Yakuri Pure Chemical Co., Japan) were used as the monomer and photoinitiator, respectively. H_2SO_4 and $FeSO_4{\cdot}7H_2O$ were used as the graft accelerator and homopolymer inhibitor, and methanol was used as the homopolymer removal solvent. DETA (Daejung Chemical Co., Korea) and $AlCl_3$ were used as the amination reagent and the reaction catalyst for transforming functional carboxyl group of the grafted AA on PP non-woven fabric into functional amine group.

The extra pure chemicals, KH_2PO_4, KNO_3, KNO_2, K_2SO_4, and KCl were used to prepare anion solution for sorption experiments. The working solutions were prepared by dissolving the chemicals in deionized water or pH buffer solution. As the pH buffer, total 0.01 M acetate buffer solution (pH 4.7) was prepared using CH_3COOH and CH_3COONa.

Polystyrene-based PA308 resin ($-N^+(CH_3)_3Cl^-$, Samyang Co., Korea) was used as a comparative adsorbent.

2.2. Preparation of PP-g-AA-Am fabric

PP-*g*-AA-Am fabrics were prepared by grafting of AA onto PP non-woven fabrics and subsequent conversion of carboxyl (–COOH) group in grafted AA to an amine (Am) group through reaction with DETA according to the procedure of our previous paper [22].

First, AA was grafted onto PP fabric by a conventional photoinduced grafting technique. The grafting solution was prepared using 70/30 (v/v)% water/methanol, and contained 15 (v/v)% AA, 0.2 (w/v)% BP, 0.2 M H_2SO_4 and 5×10^{-3} M $FeSO_4{\cdot}7H_2O$. 30 ml of grafting solution and PP non-woven fabric were placed in a glass tube and then exposed to UV light for 1 h at 60 °C. The light source used was a 400 W high-pressure mercury lamp (Miya Electric Co., Korea). After the grafting reaction, the samples were washed with methanol for 10 h in a Soxlet apparatus to remove homopolymer and dried at 60 °C to constant weight. The degree of grafting was calculated from the weight gain as described elsewhere [23]. By the graft polymerization, AA grafted PP (PP-*g*-AA) fabrics with the degree of grafting in the range of 150 ± 5% were prepared and used as the substrate for chemical modification.

Subsequently, PP-*g*-AA fabrics were immersed in DETA solution containing 4 (w/v)% of $AlCl_3$ catalyst to convert hydroxyl groups of grafted AA to amine groups. The amination reaction continued for 2–6 h at 150 °C with periodic stir. After the reaction, the aminated PP-*g*-AA (PP-*g*-AA-Am) fabrics were repeatedly washed with 1N HCl solution and deionized water to remove unreacted solution, and dried at 60 °C to constant weight. The degree of amination was calculated from the weight gain and the molar ratio between AA and DETA as described elsewhere [22,23]. By the amination reaction, PP-*g*-AA-Am fabrics with the degree of amination in the range of 36–70% were prepared and used for sorption experiments. The synthetic route and chemical structure of PP-*g*-AA-Am fabric is shown in Fig. 1.

2.3. Characterization of PP-g-AA-Am fabric

Surface characteristic of the prepared PP-*g*-AA-Am fabric was analyzed by N_2 adsorption at a relative partial pressure of 0.3 at 77 K using a surface area and porosity analyzer (Micrometrics ASAP2010, USA). The BET surface area, total pore volume and pore size distribution of the PP-*g*-AA-Am fabric were then determined. Zeta potential of the PP-*g*-AA-Am fabric was measured using a zeta potential analyzer (Otsuka ELS-Z1, Japan). Zeta potential measurements were conducted with 0.01 M NaCl solution at pH 6.0–12.0 (adjusted by HCl or NaOH). Surface morphology of the PP-*g*-AA-Am fabric was observed using a scanning electron microscope (Shimadzu S-3000N, Japan).

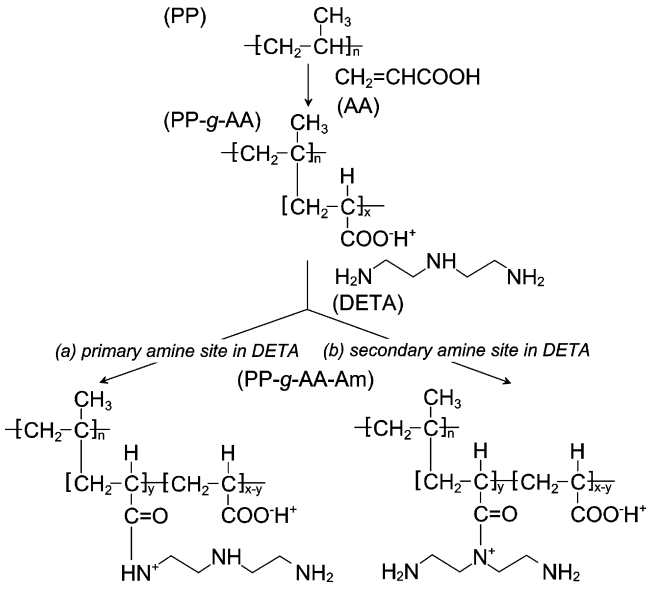

Fig. 1. The synthetic route and chemical structure of PP-*g*-AA-Am non-woven fabric.

2.4. Sorption experiments

Sorption experiments were carried out in batch conditions, in which 0.4 g of sorbent was added to 250 ml flask containing 100 ml of aqueous solution of known ion species and concentrations. The flask was then placed in an incubator shaker and shaken at 120 rpm for 24 h at 25 °C to ensure sorption equilibrium. The Initial (C_0) and equilibrium (C) anion concentrations were determined by UV spectrometer (Shimadzu UV-2401PC, Japan) and ion chromatography (Waters LC, USA). The sorbent-phase anion concentration, q (mg/g) was calculated from the anion mass balance using the following formula.

$$q = \frac{V(C_0 - C)}{W} \quad (1)$$

where V is the volume of solution (l) and W is the weight of dry sorbent (g).

To study the effect of pH on anion sorption on PP-*g*-AA-Am fabric, the experiments were carried out using the multi-anion solutions containing 1 mM of PO_4^{3-}, NO_3^-, NO_2^-, and SO_4^{2-} ion, respectively. The pH of solution was controlled to be 2.5–9.0 after the sorption equilibrium by adding HCl or NaOH solution.

The experiments for sorption selectivity were conducted using an acetic acid buffer solution (pH 4.7), which contains 100 mg/l of PO_4-P or NO_3-N paired with 0, 20, 50, 100 mg/l of Cl^-, or 1 mM of each PO_4^{3-}, NO_3^-, NO_2^-, and SO_4^{2-}, to maintain a constant pH of solution.

To evaluate the regeneration efficiency of PP-*g*-AA-Am fabric, repeated sorption-regeneration experiments were conducted using an acid washing process, in which anion-sorbed sorbent was immersed in 0.1N HCl solution and shaken for 1 h at room temperature. After complete desorption, the PP-*g*-AA-Am fabric was washed with deionized water until the pH was neutral and dried at 60 °C. The sorption-regeneration cycle was repeated 10 times and the PO_4-P sorption capacity and sorbent weight loss were measured for each cycle.

3. Results and discussion

3.1. Characteristics of PP-g-AA-Am fabric

The multipoint BET surface area, total pore volume and average pore diameter of PP-*g*-AA-Am fabric (amination 53%) were 0.6646 m^2/g, 0.00087 cm^3/g and 8.82 nm, respectively. BJH adsorption cumulative surface area of pores between 1.7 nm and 300 nm was 0.282 m^2/g. Fig. 2(a) shows the pore size distribution of the PP-*g*-AA-Am obtained by BJH method. The distribution of average pore diameter curve showed a maximum peak at an average pore diameter of about 2.0 nm. On the other hand, the cumulative amounts of micropores ($d \leq 2.0$ nm), mesopores ($2.0 < d < 50$ nm) and macropores ($d \geq 50$ nm) were 35.9%, 62.5% and 1.6%, respectively. Therefore, the PP-*g*-AA-Am fabric can be considered mixtures of micro and mesoporous materials, containing predominantly mesoporous. Fig. 2(b) shows the result of the zeta potential of PP-*g*-AA-Am fabric as a function of pH. Zeta potential decreased with increasing pH and the point of zero charge (pH_{pzc}) of PP-*g*-AA-Am fabric was at approximately pH 9.5 ± 0.1. It means that in our experimental pH conditions (pH 2.5–9.0), the surface of PP-*g*-AA-Am fabric should be always covered with positive charge. A positively charged surface site on the sorbent favors the sorption of negatively charged anionic nutrients due to electrostatic attraction.

3.2. Sorption isotherms

To study the sorption isotherm of PP-*g*-AA-Am fabric, batch PO_4-P sorption tests were conducted on fabric with degrees of amination of 36%, 53% and 70%. Fig. 3 shows the results of the equilibration of PO_4-P on PP-*g*-AA-Am fabric. The results show that the sorption capacities were increased with increasing the initial PO_4-P concentration and the degree of amination, and show the shape of type L according to the classification of Giles et al. [24]. The L-type

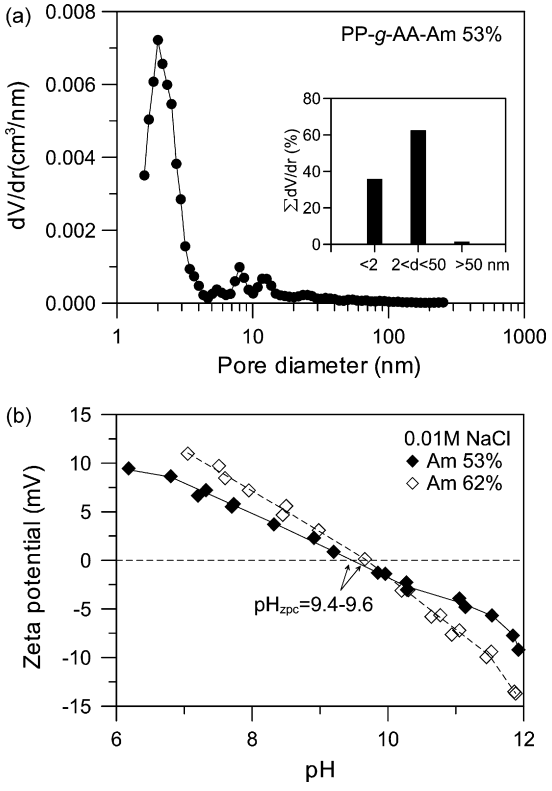

Fig. 2. Pore size distribution (a) and zeta potential (b) of PP-*g*-AA-Am non-woven fabric.

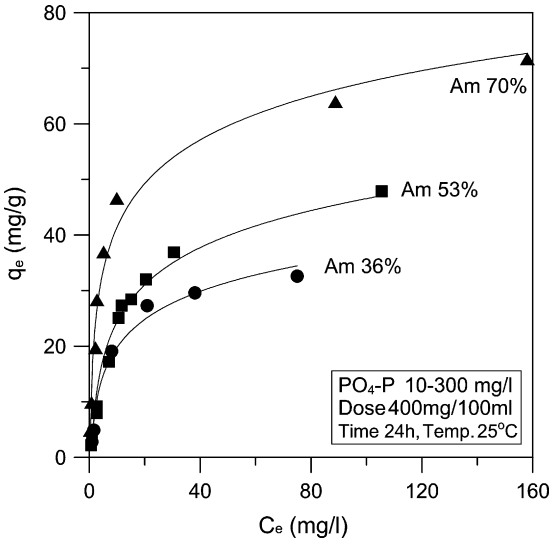

Fig. 3. Sorption isotherms of PO_4-P on PP-*g*-AA-Am non-woven fabric.

isotherm means that there is no strong competition between the solvent and the sorbate to occupy the sorbent sites.

The analysis of sorption isotherm data is important to understand how sorbates will interact with a sorbent and critical in optimizing the use of sorbent. Several models have been published in the literature to describe experimental data of the sorption isotherms. Among them, four popular sorption isotherm models, Langmuir, Freundlich, Dubinin–Radushkevich and Temkin model, were employed to interpret the experimental data.

The Langmuir isotherm is derived to model the monolayer adsorption on a homogeneous surface. The Langmuir model is given by the following equation:

$$q_e = \frac{q_m b C_e}{1 + b C_e} \tag{2}$$

where C_e is the liquid-phase concentration of the adsorbate at equilibrium (mg/l), q_e is the amount of adsorbate adsorbed at equilibrium (mg/g), q_m is the maximum adsorption capacity (mg/g), and b is the Langmuir constant related to the energy of adsorption (l/mg). This model can be linearized in two representations of Stumm and Morgan [25] and Weber [26] as follows:

$$\frac{1}{q_e} = \frac{1}{q_m} + \frac{1}{q_m b C_e} \tag{3}$$

$$\frac{C_e}{q_e} = \frac{1}{b q_m} + \frac{C_e}{q_m} \tag{4}$$

Fig. 4 shows the Langmuir isotherms for the sorption of PO_4-P on PP-*g*-AA-Am fabrics. The sorption parameters determined by using the Langmuir equation are summarized in Table 1. The results show that both representation modes of the Langmuir isotherm well described the experimental data. The values of maximum sorption capacity obtained by the representation of Stumm and Morgan were higher than of Weber, even though the differences gradually decreased with increasing the degree of amination.

The Freundlich isotherm is derived to model the multilayer adsorption on heterogeneous surfaces. The Freundlich model is given by [27]:

$$q_e = K_F C_e^{1/n} \tag{5}$$

The Freundlich equation can be linearized by logarithmic transfer:

$$\ln q_e = \ln K_F + \frac{1}{n} \ln C_e \tag{6}$$

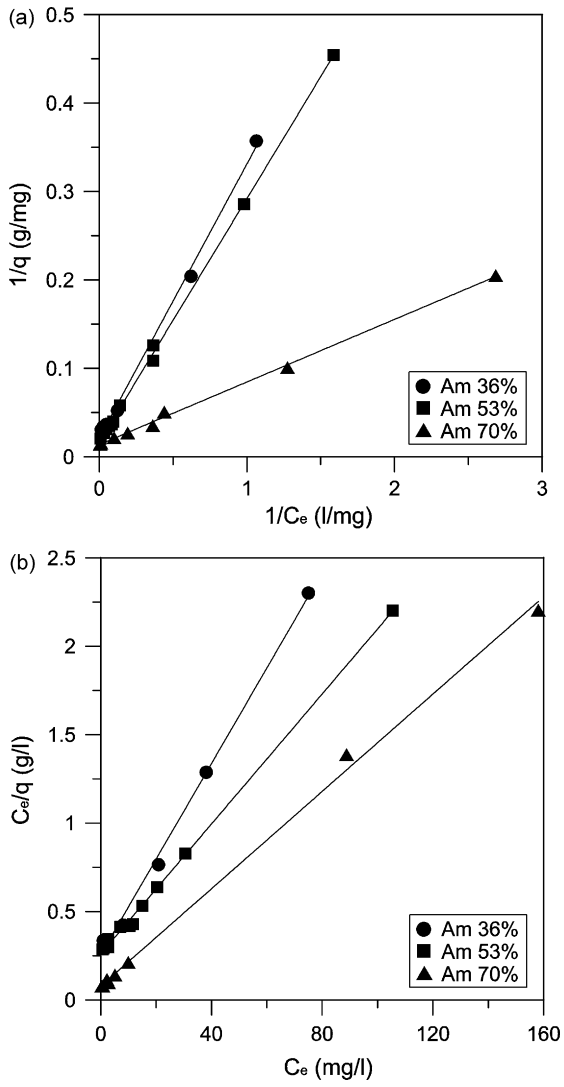

Fig. 4. Langmuir plots of PO_4-P sorption on PP-*g*-AA-Am non-woven fabric.

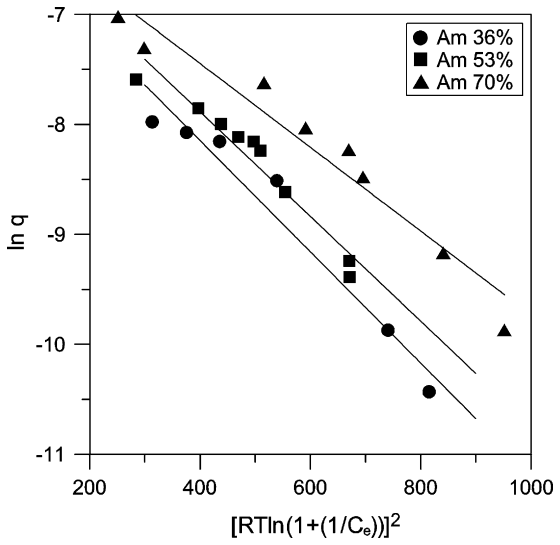

Fig. 5. D–R plot of PO_4-P sorption on PP-*g*-AA-Am non-woven fabric.

where C_e is the liquid-phase concentration of the adsorbate at equilibrium (mg/l), q_e is the amount of adsorbate adsorbed at equilibrium (mg/g), K_F is the Freundlich constant ($mg^{1-(1/n)}l^{1/n}/g$) indicative of the adsorption capacity of the adsorbent, and n is an empirical constant related to the magnitude of the adsorption driving force.

The Freundlich isotherm parameters, K_F and n values were calculated from the intercept and slope of the $\ln q_e$ versus $\ln C_e$ plots (not shown) and are summarized in Table 1. It is observed from lower regression coefficients (r^2) that the Freundlich isotherm model was less suitable for representation of the experimental data than the Langmuir isotherm model. The increase in K_F with increase of amination means that the amine group introduced to the graft chain will increase the effective sorption sites. The magnitudes of n value were in level of good ($n \geq 2$) and moderately difficult ($2 \geq n \geq 1$) favorability of sorption.

The Dubinin–Radushkevich isotherm based on the Polanyi theory is an analogue of Langmuir type in viewpoint of describing adsorption on a single type of uniform pores, but it is more general because it does not assume a homogeneous surface or constant sorption potential. The D–R model was applied to understand the sorption mechanism of PP-*g*-AA-Am fabric. The linear form of D–R model is given by [28,29]:

$$\ln q = \ln q_m - k\varepsilon^2 \quad (7)$$

where C_e is the liquid-phase concentration of the adsorbate at equilibrium (mol/l), q_e is the amount of adsorbate adsorbed at equilibrium (mol/g), q_m is the maximum adsorption capacity (mol/g), k is a constant related to the adsorption energy (mol^2/kJ^2), ε is the Polanyi potential [$RT \ln(1 + (1/C_e))$], R is the universal gas constant (kJ/mol K), and T is the temperature (K). If the plot of the $\ln q$ versus ε^2 gives a straight line, the values of q_m and k can be calculated from the intercept and slope of the straight line, respectively. The mean free energy of adsorption (E) is determined by the equation $E = (-2k)^{-0.5}$.

Fig. 5 shows the D–R isotherms for the sorption of PO_4-P on PP-*g*-AA-Am fabrics. The D–R parameters are summarized in Table 2.

The Temkin model, which also gives an information about adsorption energy, is given by [9]:

$$\frac{q_e}{q_m} = \frac{RT}{\Delta Q} \ln K_0 C_e \quad (8)$$

where ΔQ is the variation of adsorption energy (J/mol) and K_0 is the Temkin constant (l/mg). The maximum sorption capacity q_m (mg/g) obtained from the Langmuir equation represented by Stumm and Morgan was used for the plot of Temkin equation. Fig. 6 shows the Temkin isotherms for the sorption of PO_4-P on PP-*g*-AA-Am fabrics. The values of K_0 and ΔQ were calculated from the intercept

Table 1
Langmuir and Fruendlich isotherm parameters.

	Langmuir isotherm						Fruendlich isotherm		
	Stumm and Morgan			Weber			K_F (mg/g)	n	r^2
	q_m (mg/g)	b (L/mg)	r^2	q_m (mg/g)	b (L/mg)	r^2			
Am 36%	47.40	0.068	0.997	37.00	0.106	0.997	3.77	1.73	0.926
Am 53%	60.24	0.061	0.999	54.64	0.071	0.998	4.18	1.56	0.930
Am 70%	72.46	0.196	0.998	72.99	0.177	0.998	12.78	2.47	0.847

Table 2
Dubinin–Radushkevich and Temkin isotherms parameters.

	Dubinin–Radushkevich isotherm			Temkin isotherm		
	E (kJ/mol)	q_m (mmol/g)	r^2	ΔQ (kJ/mol)	K_0 (L/mg)	r^2
Am 36%	9.94	2.194	0.954	14.26	1.48	0.991
Am 53%	10.21	2.534	0.963	14.56	1.27	0.987
Am 70%	11.69	2.483	0.908	15.96	3.86	0.989

and slope of the (q_e/q_m) versus ln C_e plots and are summarized in Table 2.

Comparing regression coefficient values (r^2) given in Table 2, the Temkin model shows a better fit to the experimental data than the D–R model. The results obtained show significantly different values of sorption energy between Temkin (14.26–15.96 kJ/mol) and D–R model (9.94–11.69 kJ/mol). However, it is obvious that the highly positive value obtained from both models implies an exothermic sorption process. It is known that the magnitude of sorption energy is useful for estimating the type of sorption process. When this value is in the range of 8–16 kJ/mol, the sorption process can be explained by ion exchange [28,30–32]. Therefore, it can be concluded that ion exchange plays a significant role in the sorption process of PO_4-P onto PP-*g*-AA-Am fabric.

3.3. Sorption kinetics

The sorption kinetics of PP-*g*-AA-Am fabric and commercial anion exchange resin (PA resin) was also investigated using PO_4-P. Fig. 7 shows the amounts of PO_4-P sorbed on PP-*g*-AA-Am fabrics and PA resin as a function of contact time. All the curves exhibit similar characteristics with a rapid initial sorption process and a slower second sorption process. The comparison of the kinetic curves shows that the rate of PO_4-P sorption on PA resin was higher than those on PP-*g*-AA-Am fabrics. PO_4-P sorption by PP-g-AA-Am fabrics was ≥90% in 5 h, with sorption tending to increase continuously and gradually, reaching sorption equilibrium at around 10 h, regardless of the degree of amination. For PA resin, sorption equilibrium was reached within 60 min. It is considered that the structure of PP-*g*-AA-Am fabric was more bulky compared to the minute particle-phase PA resin, so that a longer contact time would be required to diffuse the sorbate to the internal activating site.

It is known that sorption process could be dependent on and controlled with different kinds of mechanisms, like mass transfer, diffusion control, chemical reactions and particle diffusion. In order to interpret the experimental data, Lagergren's pseudo-first-order kinetic model, pseudo-second-order kinetic model, and intraparticle diffusion model were used in this study.

The pseudo-first-order kinetic model of Lagergren is given by [33]:

$$\ln \frac{q_e - q_t}{q_e} = -k_1 t \tag{9}$$

where q_e and q_t are the amount of sorbate sorbed at equilibrium and time t (mg/g), respectively, and k_1 is the rate constant of pseudo-first-order adsorption (min^{-1}). If the plot of ln[$(q_e - q_t)/q_e$] versus t gives a straight line, the model is applicable and then the rate constant (k_1) can be determined from the slope of regression line. As shown in Fig. 8, only the first portion of sorption kinetics gives a straight fitting line. Therefore, the pseudo-first-order kinetic model cannot be used to predict the sorption kinetics of PO_4-P on PP-*g*-AA-Am fabric and PA resin for the entire sorption period, suggesting that they did not follow a first-order reaction.

On the other hand, the pseudo-second-order kinetic equation, which is more likely to predict the behavior over entire sorption period and is in agreement with chemical sorption being the rate-controlling step, is given by [34]:

$$\frac{t}{q_t} = \frac{1}{k_2 q_e^2} + \frac{t}{q_e} \tag{10}$$

where k_2 is the rate constant of pseudo-second-order adsorption (g/mg min). If the plot of t/q versus t gives a straight line, the rate constant (k_2) can be determined from the intercept and slope. The plots and regression lines of the data for the pseudo-second-order kinetic model are presented in Fig. 9. The results show that the pseudo-second-order kinetic model well predicted the experimental data clearly suggests that the PO_4-P sorption on PP-*g*-AA-Am fabrics and PA resin follows the second-order type reaction. The rate constant (k_2) and the experimental and theoretical q_e values are

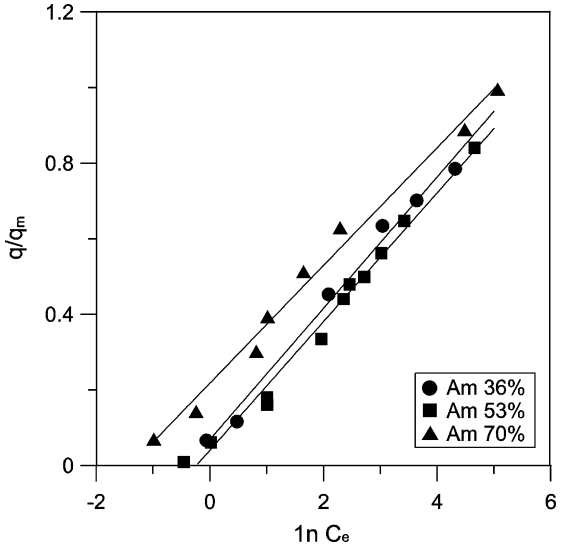

Fig. 6. Temkin plot of PO_4-P sorption on PP-*g*-AA-Am non-woven fabric.

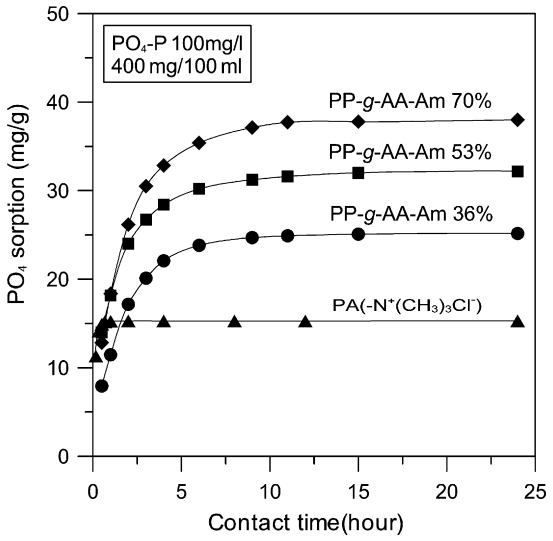

Fig. 7. Sorption rates of PO_4-P ion on PP-*g*-AA-Am non-woven fabric and PA resin.

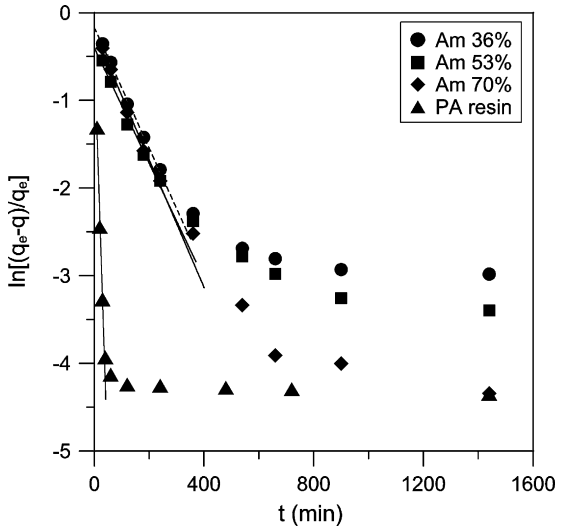

Fig. 8. Lagergren's pseudo-first-order plots for PO_4-P sorption on PP-*g*-AA-Am non-woven fabric and PA resin.

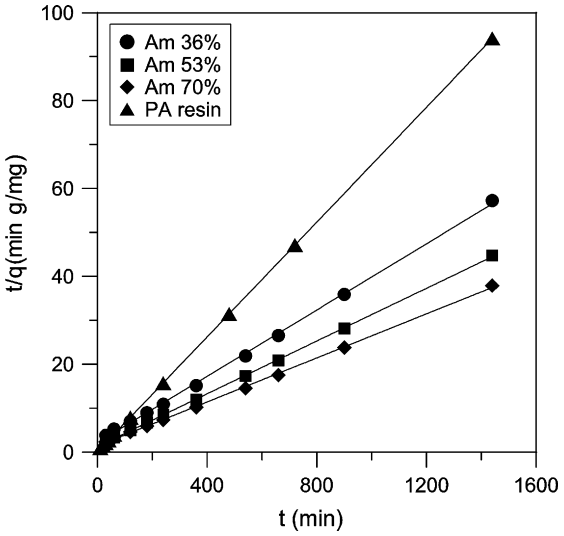

Fig. 9. Pseudo-second-order plots for PO_4-P sorption on PP-*g*-AA-Am non-woven fabric and PA resin.

given in Table 3. This result can be expected because the ordinary type of exchange processes is more rapid and controlled mainly by diffusion, whereas, those in chelating exchanger are slower and controlled either by particle diffusion mechanisms or by a second-order chemical reaction [35]. The k_2 values of PP-*g*-AA-Am fabric were approximately 35 times smaller than that of PA resin.

Intraparticle diffusion model of Weber and Morris [36] is given by:

$$q_t = k_{id}\, t^{1/2} + C \quad (11)$$

where q_t is the amount of sorbate sorbed at time t (mg/g), and k_{id} is the rate constant of intraparticle diffusion (g/mg min). Fig. 10

Table 3
Second-order kinetic rate constants.

	q_e (exp.) (mg/g)	q_e (theor.) (mg/g)	k_2 (g/mg min)	r^2
PA resin	15.30	15.31	6.13×10^{-2}	1.000
Am 36%	25.16	26.52	6.58×10^{-4}	0.999
Am 53%	32.19	33.33	7.14×10^{-4}	0.999
Am 70%	38.13	39.92	4.56×10^{-4}	0.999

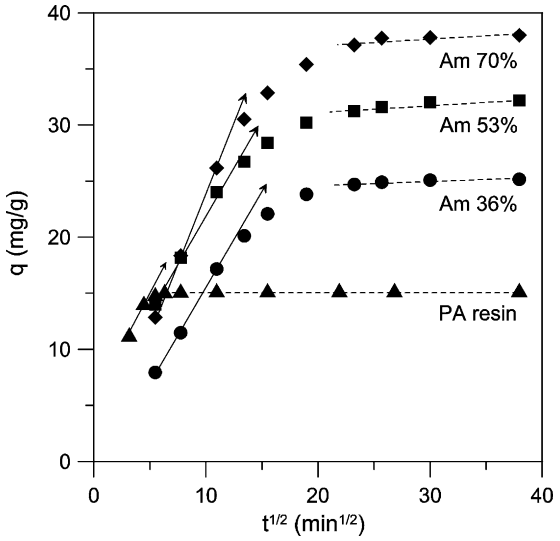

Fig. 10. Intraparticle diffusion plots for PO_4-P sorption on PP-*g*-AA-Am non-woven fabric and PA resin.

shows the plots of q_t versus $t^{1/2}$ for PO_4-P onto PP-*g*-AA-Am fabric and PA resin. The plots exhibited two linear phases that an initial linear portion ended with a smooth curve followed by second linear portion. The dual linear plots indicate that two intraparticle diffusion steps occurred in the sorption processes. The similar dual or multiple linear plots were also reported in the literatures [9,21,37,38]. Also, it has been noticed in many studies that boundary layer diffusion or surface sorption is dominant during the initial sorbate uptake, then gradually the sorption rate becomes controlled by intraparticle or pore diffusion after the sorbent external surface is loaded with the sorbate. Considering the pore size distribution of PP-*g*-AA-Am fabric shown in Fig. 2(a), however, it is also possible that the first linear portion was attributed to the mesopore diffusion and the second linear portion to micropore diffusion. The intraparticle diffusion parameters calculated from the slopes and intercepts of initial and second linear portion are given in Table 4. The intraparticle diffusion coefficient $k_{id,2}$ values for second linear portion of plots are much lower than the $k_{id,1}$ values for first linear portion of plots, thus the second linear step is the rate-limiting step in the sorption process. However, the fact that neither plots passed through the origin indicates that although intraparticle diffusion was involved in the sorption process, it was not the only rate-limiting step for the whole sorption process [39], and that other sorption mechanisms were potentially involved in the sorption process. On the other hand, it is known that the intercept of the plot gives an idea about boundary layer effect in the sorption process. The larger the value of the intercept, the greater is the contribution of the boundary layer effect in the rate-limiting step [39,40]. Namely the intercept reflects the abundance of sorbate sorbed on boundary layer. The intercept values C_2 obtained for second linear portions of the plots of PP-*g*-AA-Am fabrics were increased with increasing the degree of amination.

3.4. Effect of pH

The pH of solution is an important parameter in the sorption process because the speciation of anions and the surface characteristics of the sorbent are influenced by the pH value. To study the effect of solution pH on anionic nutrient sorption by PP-*g*-AA-Am fabric, the experiment was conducted with an equimolar multi-anion solution at different pH values (2.5–9.0). Fig. 11 shows the results of the equilibrium uptake of each NO_2^-, NO_3^-, PO_4^{3-} and SO_4^{2-} ion onto PP-*g*-AA-Am fabric as a function of

Table 4
Intraparticle diffusion model parameters.

	First linear portion			Second linear portion		
	$k_{id,1}$ (mg/g min$^{0.5}$)	C_1 (mg/g)	r^2	$k_{id,2}$ (mg/g min$^{0.5}$)	C_2 (mg/g)	r^2
PA resin	1.186	0.720	0.999	0.001	15.26	0.994
Am 36%	1.446	0.399	0.988	0.055	23.42	0.969
Am 53%	1.827	3.995	0.999	0.061	29.98	0.913
Am 70%	2.254	0.786	0.995	0.058	35.87	0.886

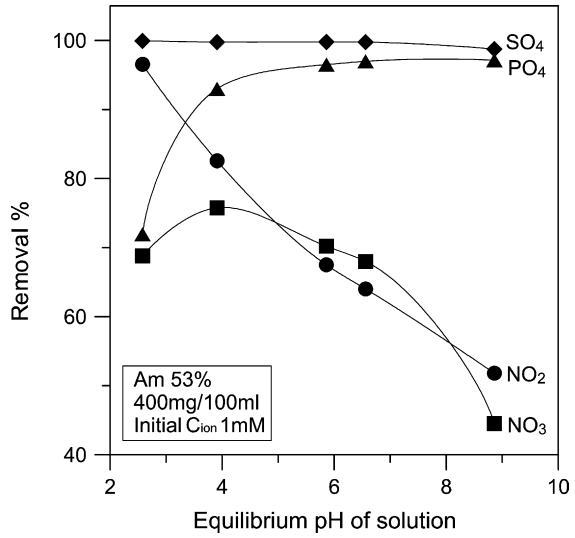

Fig. 11. Effect of pH on the sorption of anions on PP-*g*-AA-Am non-woven fabric.

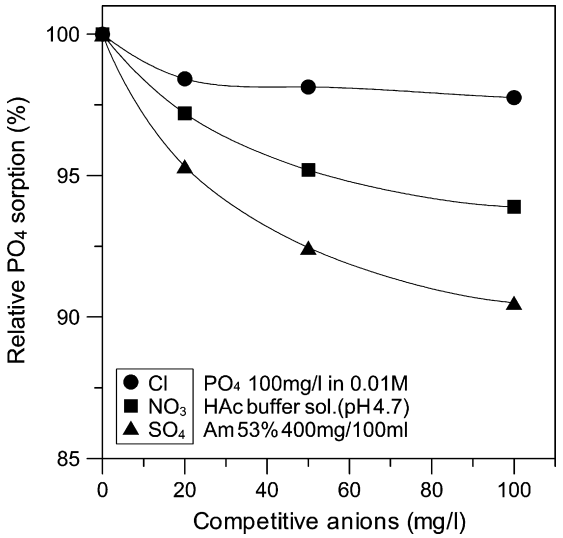

Fig. 13. Effect of competitive anions on PO_4-P sorption onto PP-*g*-AA-Am non-woven fabric.

the equilibrium pH of solution. As shown in Fig. 11, the equilibrium uptake of NO_3-N reached the highest value at near pH 4 and then decreased with increasing pH, while the equilibrium uptake of NO_2-N systematically decreased with increasing pH of solution. It may be interpreted by change of sorbent surface charge or ion competition. As pH of solution increased, the number of positively charged surface sites decreased, which is unfavorable to sorption of negatively charged anion. Ion competition is also a point to be considered because multi-anion solution was used in the experiment. This may be one of the reasons for the decreased NO_3-N sorption at pH <4.0, and even for the decreasing NO_2-N and NO_3-N sorption with increasing pH ≥4.0. However, they could not explain the pH effect on the sorption of PO_4-P and SO_4^{2-}. The equilibrium uptake of PO_4-P onto PP-*g*-AA-Am fabric increased with increasing pH of solution. Optimum pH for PO_4-P sorption was observed in the pH ≥4.0. Lower sorption of PO_4-P in the pH ≤4.0 could be explained by the increasing univalent phosphate ion and non-ionized phosphoric acid ($pK_{H_3PO_4} = 2.12$) with decreasing pH. With increasing pH, the phosphates like $H_2PO_4^-$, HPO_4^{2-}, and PO_4^{3-} became major species, which are more favorable to sorption by PP-*g*-AA-Am fabric. In contrast, the equilibrium uptake of SO_4^{2-} ion tended to

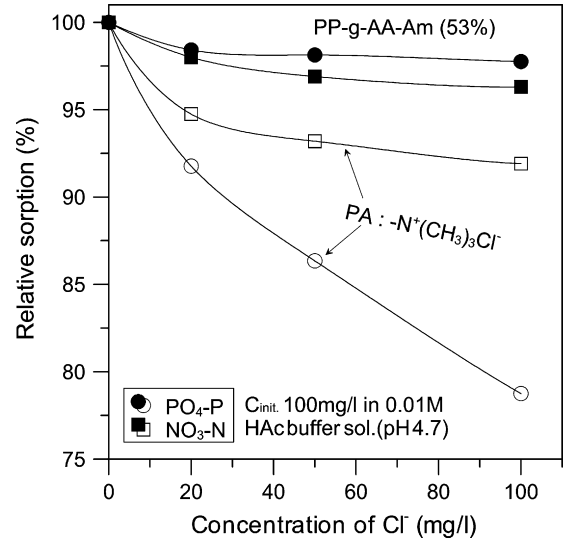

Fig. 12. Effect of Cl^- ion on PO_4-P and NO_3-N sorption onto PP-*g*-AA-Am non-woven fabric and PA resin.

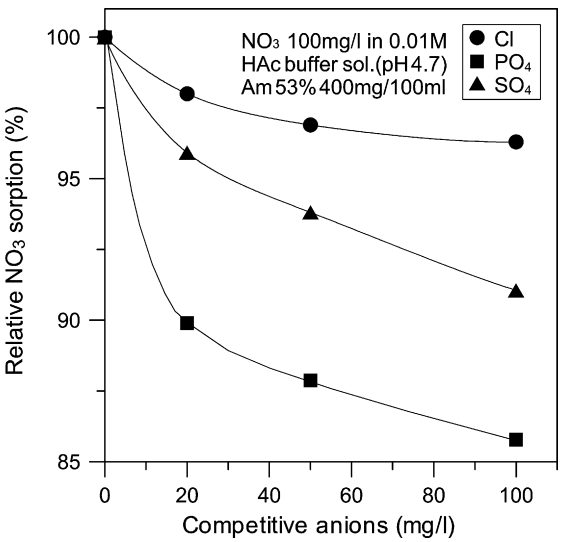

Fig. 14. Effect of competitive anions on NO_3-N sorption onto PP-*g*-AA-Am non-woven fabric.

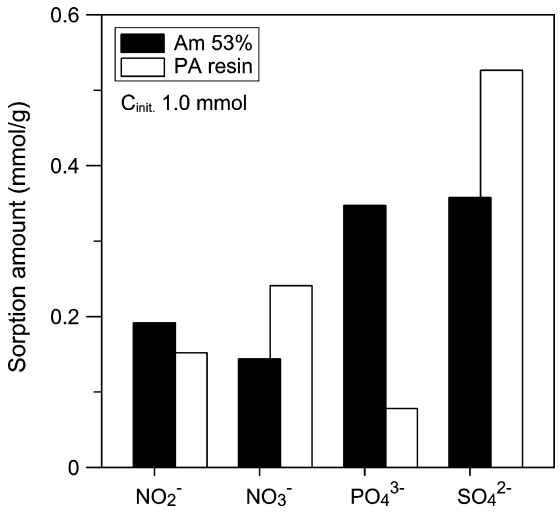

Fig. 15. Ion selectivity of PP-*g*-AA-Am non-woven fabric and PA resin in the presence of equimolar anions.

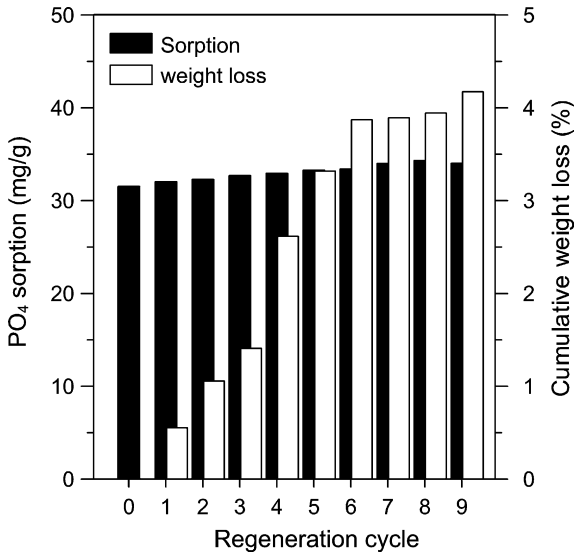

Fig. 16. Regeneration efficiency of PP-*g*-AA-Am non-woven fabric by 0.1N HCl washing.

stabilize into a constant value regardless of pH and thus, indicates that it was not affected by the pH of solution in range of 2.5–9.0.

3.5. Effect of competitive anions

One of the major problems which limit the wide application of ion exchange method to eliminate pollutants is the ion selectivity for an ion exchange resin. Fig. 12 shows the effects of Cl^-, which is a common replaceable ion on the surface of sorbents used, on the uptake of PO_4-P and NO_3-N onto PP-*g*-AA-Am fabric and commercial PA resin. As shown in Fig. 12, it is obvious that PO_4-P and NO_3-N uptakes decreased with an increase in the concentration of Cl^-. Comparing with PA resin, however, the PP-*g*-AA-Am fabric showed only a slight decrease in uptake of PO_4-P as the concentration of Cl^- increases. Same result was observed for NO_3-N in the presence of Cl^-. It is evident that the PP-*g*-AA-Am fabric had a good affinity for PO_4-P, even for NO_3-N, over Cl^-. Figs. 13 and 14 show the effect of the other competing anions on the uptakes of PO_4-P and NO_3-N (C_0 = 100 mg/l) onto PP-*g*-AA-Am fabric. The effect of Cl^- was plotted again in the Figs. 13 and 14 for comparison. It is obvious that PO_4-P and NO_3-N uptake was insensitive in the presence of Cl^- (2–3% decrease) as compared to the presence of other anions. Meanwhile, PO_4-P uptake was considerably decreased in the presence of NO_3^- (6% decrease) and SO_4^{2-} (9% decrease). Same results were observed for NO_3^- in the presence of SO_4^{2-} (9% uptake decrease) and PO_4-P, which predominately exists as $H_2PO_4^-$ in our experimental condition (14% uptake decrease).

The sorption competitiveness among coexisting anions for PP-*g*-AA-Am fabric was studied in the presence of equimolar anions. The results are presented in Fig. 15 and compared with those obtained for PA resin at the same experimental conditions. As shown in Fig. 15, the sorption selectivity of PP-*g*-AA-Am fabric for anions increased in the order: $SO_4^{2-} \geq PO_4$-P > NO_2^- > NO_3^-, where PO_4-P exists predominately as univalent species $H_2PO_4^-$ in our experimental condition (pH 4.7). In contrast, the selectivity order of PA resin increased in the order: SO_4^{2-} > NO_3^- > NO_2^- > PO_4-P.

From these results, it could be concluded that PP-*g*-AA-Am fabric had a significantly high affinity for PO_4-P, and its sorption capacity was not significantly affected by the presence of competitive anions. Furthermore, the fact that the sorption capacity of PP-*g*-AA-Am fabric for PO_4-P was approximately three times higher than the commercial PA resin, suggests the possibility of PP-*g*-AA-Am fabric as a phosphate selective ion exchanger.

3.6. Regeneration efficiency

To investigate the regeneration efficiency of PP-*g*-AA-Am fabric, repeated sorption-regeneration experiments were performed.

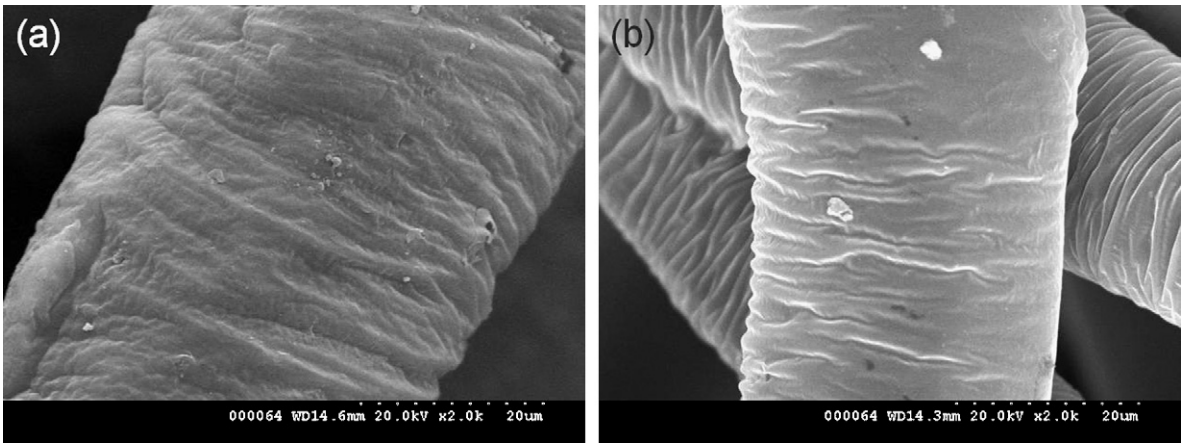

Fig. 17. SEM images of PP-*g*-AA-Am non-woven fabric (a) and after regenerated 10 times with 0.1N HCl (b).

As shown in Fig. 16, the sorption capacity retained almost constant regardless of the number of regeneration cycles. On the other hand, the weight of PP-*g*-AA-Am fabric continuously decreased with the number of regeneration cycles, but the weight loss range was less than 5%, even after 10 regeneration cycles. Fig. 17 shows SEM images of the PP-*g*-AA-Am fabric surface before use and after 10 regeneration cycles. The regenerated PP-*g*-AA-Am fabric exhibits less roughness and more crumpled structure on the surface compared to the virgin fabric. It is probably due to abrasive or washing loss of impurities and physical deformation on repeated swelling and shrinking of grafting layers during the regeneration processes. As a result, PP-*g*-AA-Am fabric could be regenerated by a simple acid washing process without lowering the sorption capacity or durability and used more than 10 times maintaining the same sorbent quality.

4. Conclusions

The sorption kinetic data for uptake of PO_4-P ion onto PP-*g*-AA-Am fabric indicated that sorption occurred with at least two interconnected processes and seemed to reach equilibration in around 10 h. The sorption process was found to follow a pseudo-second-order kinetic model and controlled by both external and intraparticle diffusions. The sorption of PO_4-P on PP-*g*-AA-Am fabric could be accurately described by Langmuir isotherm. Maximum sorption capacities obtained by the Langmuir equation increased from 37 to 73 mg/g as the degree of amination increases from 36% to 70%. Sorption energies for PO_4-P, determined using D–R model and Temkin model, were positive in the range of 9–16 kJ/mol. Therefore, the sorption mechanism for PP-*g*-AA-Am fabric could be explained with an ion exchange process. The uptake of PO_4-P by PP-*g*-AA-Am fabric increased with increasing the pH of solution and its optimum pH region was $\geq$4.0. Meanwhile, the uptakes of NO_3-N and NO_2-N were high in weak and strong acidic pH regions, respectively, and tended to decrease with increasing the pH of solution. The selectivity of PP-*g*-AA-Am fabric in the presence of equimolar anions and at pH 4.7 increased in the order: $SO_4^{2-} \geq PO_4^{3-} > NO_2^- > NO_3^-$. However, the uptake of PO_4-P by PP-*g*-AA-Am fabric was not significantly affected by the presence of SO_4^{2-}. The effect of Cl^- was also negligible on the uptake of PO_4-P and NO_3-N. The PP-*g*-AA-Am fabric could be regenerated by a simple acid washing process without lowering the sorption capacity or durability and could be used more than 10 times while retaining the same sorption capacity. The results of this present investigation suggest that the PP-*g*-AA-Am fabric could be used as a phosphate selective ion exchanger.

Acknowledgement

This work was supported by the Korea Research Foundation Grant funded by the Korean Government (MOEHRD) (KRF-2007-359-D00009 (I00036)).

References

[1] W. Saktaywin, H. Tsuno, H. Nagare, T. Soyama, J. Weerapakkaroon, Advanced sewage treatment process with excess sludge reduction and phosphorus recovery, Water Res. 39 (2005) 902–910.
[2] P. Gogate, B. Aniruddlha, Review of imperative technologies for wastewater treatment. II. Hybrid methods, Adv. Environ. Res. 8 (2004) 553–597.
[3] A. Genz, A. Kornmuller, M. Jekel, Advanced phosphrous removal from membrane filtrates by adsorption on activated aluminium oxide and granulated ferric hydroxide, Water Res. 38 (2004) 3523–3530.
[4] K.M. Yeon, J.S. Park, C.H. Lee, S.M. Kim, Membrane coupled high-performance compact reactor: a new MBR system for advanced wastewater treatment, Water Res. 39 (2005) 1954–1961.
[5] N.M. Al-Bastaki, Performance of advanced methods for treatment of wastewater: UV/TiO_2, RO and UF, Chem. Eng. Process. 43 (2004) 935–940.
[6] G. Chen, Electrochemical technologies in wastewater treatment, Separ. Purif. Technol. 38 (2004) 11–41.
[7] S. Espulgas, S. Contreras, D.F. Ollis, Engineering aspects of the integration of chemical and biological oxidation: simple mechanistic models for the oxidation treatment, J. Environ. Eng. 130 (2004) 967–974.
[8] S.H. Lin, C.D. Kiang, Combined physical, chemical and biological treatments of wastewater containing organics from a semiconductor plant, J. Hazard. Mater. B 97 (2003) 159–171.
[9] O. Hamdaoui, Batch study of liquid-phase adsorption of methylene blue using cedar sawdust and crushed brick, J. Hazard. Mater. 135 (2006) 264–273.
[10] W.D. Henry, D. Zhao, A.K. Sengupta, C. Lange, Preparation and characterization of a new class of polymeric ligand exchangers for selective removal of trace contaminants from water, React. Funct. Polym. 60 (2004) 109–120.
[11] S. Cornelia, H. Jurgen, H.H. Wolfgang, Adsorption of the surface complex formation model to ion exchange equilibria(V): adsorption of heavy metal salts onto weakly basic anion exchangers, React. Funct. Polym. 49 (2001) 117–132.
[12] N. Özutürk, T.E. Bektaş, Nitrate removal from aqueous solution by adsorption onto various materials, J. Hazard. Mater. 112 (2004) 155–162.
[13] B.U. Bae, Y.H. Jung, W.W. Han, H.S. Shin, Improved brine recycling during nitrate removal using ion exchange, Water Res. 36 (2002) 3330–3340.
[14] C. Luengo, M. Brigante, J. Antelo, M. Avena, Kinetics of phosphate adsorption on goethite: comparing batch adsorption and ATR-IR measurements, J. Colloid Interface Sci. 300 (2006) 511–518.
[15] R. Chitrakar, A. Tezuka, A. Sonoda, K. Sakane, K. Ooi, T. Hirotsu, Phosphate adsorption on synthetic goethite and akaganeite, J. Colloid Interface Sci. 298 (2006) 602–608.
[16] J. Antelo, M. Avena, S. Fiol, R. López, F. Arce, Rheological behavior of organic suspensions of fluorapatite, J. Colloid Interface Sci. 285 (2005) 476–486.
[17] S. Tanada, M. Kabayama, N. Kawasaki, T. Sakiyama, T. Nakamura, M. Araki, T. Tamura, Removal of phosphate by aluminum oxide hydroxide, J. Colloid Interface Sci. 257 (2003) 135–140.
[18] T.L. Eberhardt, S.-H. Min, J.S. Han, Phosphate removal by refined aspen wood fiber treated with carboxymethyl cellulose and ferrous chloride, Bioresour. Technol. 97 (2006) 2371–2376.
[19] M. Boumediene, D. Achour, Denitrification of the underground waters by specific resin exchange of ion, Desalination 168 (2004) 187–194.
[20] S. Samatya, N. Kabay, Ü. Yüksel, M. Arda, M. Yüksel, Removal of nitrate from aqueous solution by nitrate selective ion exchange resins, React. Funct. Polym. 66 (2006) 1206–1214.
[21] L. Ruixia, G. Jinlong, T. Hongxiao, Adsorption of fluoride, phosphate, and arsenate ions on a new type of ion exchange fiber, J. Colloid Interface Sci. 248 (2002) 268–274.
[22] H.J. Park, C.K. Na, Preparation of anion exchanger by amination of acrylic acid grafted polypropylene nonwoven fiber and its ion-exchange property, J. Colloid Interface Sci. 301 (2006) 46–54.
[23] T. Kawai, K. Saito, K. Sugita, T. Kawakami, J. Kanno, A. Katakai, N. Seko, T. Sugo, Preparation of hydrophilic amidoxime fibers by cografting acrylonitrile and methacrylic acid from an optimized monomer composition, Radiat. Phys. Chem. 59 (2000) 405.
[24] C.H. Giles, D. Smith, A. Smith, A general treatment and classification of the solute adsorption isotherm. I. Theoretical, J. Colloid Interface Sci. 47 (1974) 755–765.
[25] W. Stumm, J.J. Morgan, Aquatic Chemistry, 2nd ed., Wiley Interscience, John Wiley & Sons, 1981.
[26] J. Weber Jr., in: R.L. Metcalf, J.N. Pitts (Eds.), Adsorption Physicochemical Processes for Water Quality Control, Wiley Interscience, NY, 1972, pp. 199–259.
[27] H.M.F. Freundlich, Over the adsorption in solution, J. Phys. Chem. 57 (1906) 385–470.
[28] M.M. Dubinin, E.D. Zaverina, L.V. Radushkevich, Sorption and structure of active carbons. I. Adsorption of organic vapors, Zh. Fiz. Khim. 21 (1947) 1351–1362.
[29] A. Kilislioğlu, B. Bilgin, Thermodynamic and kinetic investigations of uranium adsorption on amberlite IR-118H resin, Appl. Radiat. Isot. 50 (2003) 155–160.
[30] R.E. Terybal, Mass-Transfer Operations, 3rd ed., McGraw Hill, 1981.
[31] A. Sarı, M. Tuzen, D. Cıtak, M. Soylak, Adsorption characteristics of Cu(II) and Pb(II) onto expanded perlite from aqueous solution, J. Hazard. Mater. 148 (2007) 387–394.
[32] A.E. Nemr, Potential of pomegranate husk carbon for Cr(VI) removal from wastewater: kinetic and isotherm studies, J. Hazard. Mater. (2008), doi:10.1016/j.jhazmat.2008.03.093.
[33] S. Lagergren, About the theory of so-called adsorption of soluble substances, Kunglia Svenska Vetenskapsakademiens Handlingar 24 (1898) 1–39.
[34] Y.S. Ho, G. McKay, Pseudo-second order model for sorption process, Proc. Biochem. 34 (1999) 451–465.
[35] C. Kantipuly, S. Katragadda, A. Chow, H.D. Gesser, Chelating polymers and related supports for separation and preconcentration of trace metals, Talanta 37 (1990) 491–517.
[36] W.J. Weber, J.C. Morris, Kinetics of adsorption of carbon from solutions, J. Sanit. Eng. Div. Am. Soc. Eng. 89 (1963) 31–59.
[37] V.C. Taty-Costodes, H. Fauduct, C. Porte, A. Delacroix, Removal of Cd(II) and Pb(II) ions, from aqueous solutions, by adsorption onto sawdust of *Pinus sylvestris*, J. Hazard. Mater. 105 (2003) 121–142.
[38] S.V. Mohan, N.C. Rao, J. Karthikeyan, Adsorptive removal of direct azo dye from aqueous phase onto coal based sorbents: a kinetic and mechanistic study, J. Hazard. Mater. 90 (2002) 189–204.
[39] B. Acemioglu, Batch kinetics study of sorption of methylene blue by perlite, Chem. Eng. J. 106 (2004) 73–81.
[40] D. Mehmet, O. Yasemin, A. Mahir, Adsorption kinetics and mechanism of cationic methyl violet and methylene blue dyes onto sepiolite, Dyes Pigments 75 (2007) 701–713.